Focused fluorescence excitation with time-reversed ultrasonically encoded light and imaging in thick scattering media

LETTER

Focused fluorescence excitation with time-reversed ultrasonically encoded light and imaging in thick scattering media

Puxiang Lai[1]**, Yuta Suzuki**[1]**, Xiao Xu**[1] **and Lihong V Wang**

Optical Imaging Laboratory, Department of Biomedical Engineering, Washington University in St Louis, St Louis, MO 63130-4899, USA

E-mail: lhwang@wustl.edu

Abstract

Scattering dominates light propagation in biological tissue, and therefore restricts both resolution and penetration depth in optical imaging within thick tissue. As photons travel into the diffusive regime, typically 1 mm beneath human skin, their trajectories transition from ballistic to diffusive due to the increased number of scattering events, which makes it impossible to focus, much less track, photon paths. Consequently, imaging methods that rely on controlled light illumination are ineffective in deep tissue. This problem has recently been addressed by a novel method capable of dynamically focusing light in thick scattering media via time reversal of ultrasonically encoded (TRUE) diffused light. Here, using photorefractive materials as phase conjugate mirrors, we show a direct visualization and dynamic control of optical focusing with this light delivery method, and demonstrate its application for focused fluorescence excitation and imaging in thick turbid media. These abilities are increasingly critical for understanding the dynamic interactions of light with biological matter and processes at different system levels, as well as their applications for biomedical diagnosis and therapy.

S Online supplementary data available from stacks.iop.org/LPL/10/075604/mmedia

(Some figures may appear in colour only in the online journal)

1. Introduction

Optical methods play increasingly important roles in biomedical imaging, manipulation and therapy [1, 2]. Many of these methods rely on the ability to deliver light to the investigation sites with high spatial resolution. In soft biological tissue, elastic scattering dominates the light–matter interaction, and scrambles the propagation of light beyond superficial depths [3]. It therefore seems an impossible task to deliver or track photons with prescribed spatial and temporal precision in deep tissue using a forward problem approach. On the other hand, the deterministic nature of light propagation, coupled with its time symmetry, makes it possible to reverse [4, 5] or even shape [6–8] the photon propagation paths in an inverse problem approach.

Expanding on this approach, and with the aid of a focused ultrasound (US) beam serving as a virtual internal guide star, Xu *et al* [9] achieved dynamic focusing of light into arbitrary locations inside a scattering medium using time-reversed ultrasonically encoded (TRUE) light. In this two-step method, diffused coherent light is first spectrally encoded at the US focus inside a scattering medium. Optical focusing into the

[1] Equal contribution.

medium is accomplished by selectively phase conjugating, or time reversing, the ultrasonically encoded light, using a phase conjugate mirror (PCM).

Two versions of TRUE optical focusing technology are in development. The first approach, an analogue version, uses a photorefractive material as the PCM [9–11]. The second approach, a digital version, uses digital holography to resolve the wavefront of the ultrasonically encoded light, and uses a spatial light modulator (SLM) to construct the time-reversed light. This implementation has recently been demonstrated by Wang *et al* [12] and Si *et al* [13]. While both versions are capable of focusing light into thick scattering media, notable differences exist as a result of the specific technical implementations, and have significant bearings on the applications.

Several factors determine the efficacy of TRUE focusing, hence its enhancement of optical imaging in deep tissue. The most important figure of merit is the focus-to-background ratio (FBR), which characterizes how well light can be focused in spite of the residual speckle background due to the incomplete time reversal process in a practical setting. For analogue TRUE focusing, a photorefractive PCM can have a holographic recording area of >2500 mm^2, and a recording density of 5000–10 000 pixels mm^{-1} [14], yielding a total of $>6.25 \times 10^{10}$–2.5×10^{11} pixels. In comparison, the state-of-the-art SLM used in a digital system has only 1920×1280 pixels. The analogue system's ability to reconstruct the focusing wavefront with four to five orders more independent optical modes enables a more complete phase conjugation and a higher FBR, which is proportional to the number of controlled independent optical modes (pixels) in the reconstructed wavefront (N), but inversely proportional to the number of optical modes within the US focus (M), i.e. FBR $\propto N/M$ [8, 12]. In the diffusion regime, the independent optical modes can be estimated as fully developed speckles, and have dimensions of about $(\lambda/2)^3$, where λ is the optical wavelength in the medium. Therefore, the constraint of FBR > 1 sets an upper limit of the size of the US focus for both analogue and digital TRUE focusing. Because of the vastly different number of pixels, an analogue TRUE focusing system is capable of delivering light to a much bigger—and usually much deeper, due to more modulated photons—focus than a digital TRUE system. The speed of TRUE focusing is another important parameter, especially in the context of *in vivo* biomedical imaging, when optical time reversal has to be executed within the speckle correlation time, which is usually of the order of milliseconds [15, 16]. In analogue TRUE focusing, time reversal is implemented in a photorefractive PCM, whose response time is currently around 200 ms [9, 10] but can be faster than 1 ms under pulsed laser illumination [17]. In a digital system, however, time reversal comprises a cascade of processes, all of which contribute to the overall response time of the system, currently up to 6.7 s [12]. The bottleneck is data capture and transfer among the holographic recording camera, the controller/computer and the SLM. In theory, the speed can be increased with better integration of the digital modules, which requires further development. A third determining factor is the attainable optical gain, which characterizes how

much optical energy can be delivered in the phase conjugated light relative to the original ultrasonically encoded light energy. Although special measures can be taken to enhance the gain [18], it is usually less than unity in analogue TRUE focusing, where dynamic holographic readout simultaneously erases the existing hologram on the PCM. By contrast, in a digital TRUE focusing system, the generation of the phase conjugated light by an SLM is physically decoupled from the holographic recording device (CCD or CMOS camera). Thus the power of the phase conjugated light is proportional to the power of the reference beam illuminating the SLM and is restricted only by the damage threshold of the SLM. Large optical gains of up to 5×10^4 can be achieved [12]. However, as our letter will show, the finite analogue TRUE focusing gain does not prevent its application in fluorescence imaging in turbid media. Finally, the simplicity of the analogue system reduces its implementation cost and operational complexity, making it a desirable choice for many applications.

2. Methods and results

Figures 1(a) and (b) show the two stages of optical focusing and localized fluorescence excitation in a turbid medium with TRUE light, and figure 1(c) is a schematic of the analogue TRUE setup. In the holographic recording stage (figure 1(a)), a focused US beam (with a frequency of f_{US}) modulates the diffusively propagating sample beam in a turbid medium. The incident light beam (S), shifted to the frequency of f_0–f_{US}, has an intensity of 150–203 mW cm^{-2}, conforming with the ANSI laser safety limit for skin irradiation [19]. The output diffused light from the turbid medium is collected onto a PCM based on a photorefractive polymer film or crystal in this study. A reference beam, $R(f_0)$ (10 mW cm^{-2}), selectively interferes with the ultrasonically modulated photons, and forms a stationary interference pattern, or a hologram, inside the photorefractive material. In the subsequent holographic reading stage (figure 1(b)), a reading beam, R*(f_0) (140 mW cm^{-2}), propagates along the direction opposite to R, generating a phase conjugated beam from the PCM. Due to the reversibility of light propagation, the phase conjugated beam travels 'reversely' into the turbid medium and converges at the US focus, achieving localized excitation of the fluorescent object.

The direct observation of TRUE focus in a thick turbid medium is not possible if the focal spot dwells completely inside a highly scattering medium. To resolve this issue, we used a three-layered gel sample, composed of two turbid layers sandwiching a central clear layer, as shown in figure 2(a). The turbid layers were 4 and 5 mm thick, respectively. They were made from a gel mixture of de-ionized water, 10% (by weight) porcine gelatin (Sigma-Aldrich) and 0.5% Intralipid (Fresenius Kabi) to achieve a reduced scattering coefficient $\mu'_s = 0.5$ mm^{-1}. The clear layer was made from the gel mixture of de-ionized water and porcine gelatin only. At its center, a 20 mm $\times$ 1 mm $\times$ 1 mm (along $X \times Y \times Z$, respectively) fluorescent bar was embedded, containing quantum dots (QSA-600-2, Ocean Nanotech) as fluorophores used with a concentration of
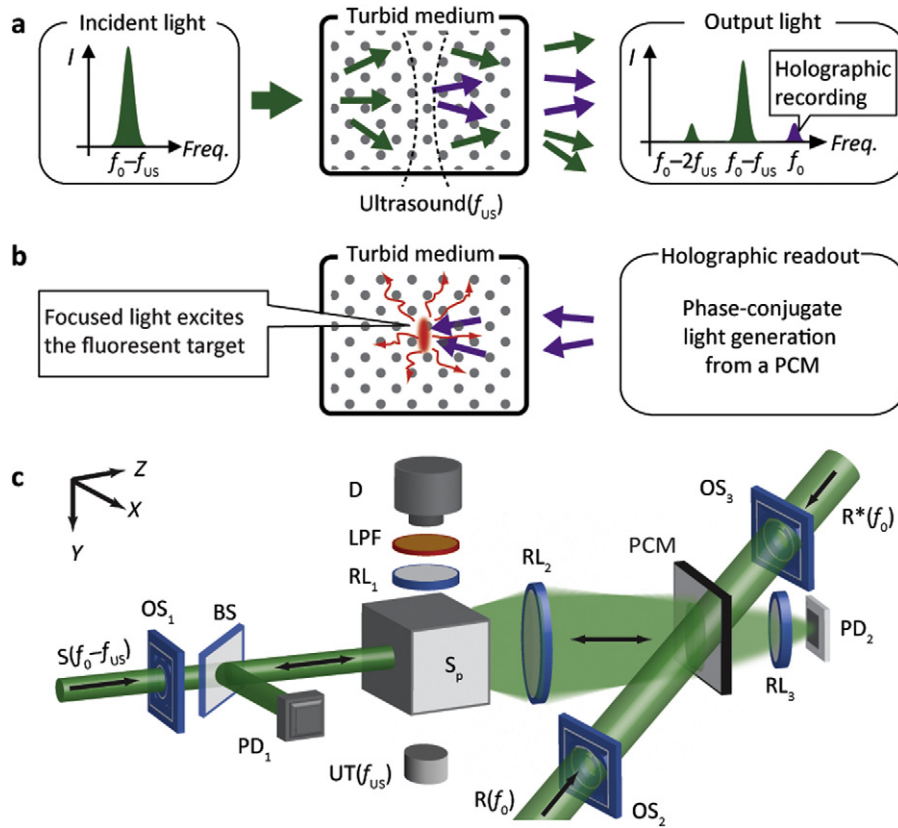
Figure 1. Schematic of focused fluorescence excitation in turbid media with TRUE light. (a) Holographic recording of ultrasound-modulated photons. (b) Phase conjugated copies of ultrasound-modulated photons travel 'time reversely' to the US focus and excite the fluorescent target. (c) The essential components of the experimental setup: BS, beam splitter; D, fluorescence detector (a CCD camera or an avalanche photodiode, APD, in this study); LPF, long-pass filter; OS_{1-3}, optical shutters; PCM, phase conjugation mirror; $PD_{1,2}$, photodiodes; R, reference beam; R^*, reading beam; RL_{1-3}, relay lenses; S, incident sample beam; UT, ultrasound transducer; *XYZ*, system coordinates.

0.26 μM. The TRUE focusing was targeted on the fluorescent bar, and our three-layered sample arrangement enabled direct observation of the excited fluorescent light distribution, while still mimicking a turbid environment. A CCD camera (iStar 734, Andor Technology) was mounted above the sample and visualized the distribution of excited fluorescent light through a long-pass filter (FGL590S, Thorlabs), which rejects the excitation light. An ultrasound transducer (UT, Panametrics A381S, Olympus) provided a 3.5 MHz continuous US beam with a focal full width at half maximum (FWHM) of 1.2 mm and a peak-to-peak focal pressure of 1.1 MPa. To reduce the speckle decorrelation caused by the US beam, the back turbid layer of the sample was mounted separately, mechanically decoupling it from the first two layers. For TRUE focusing visualization, a sufficiently long CCD exposure time was required to overcome dark noise. Therefore we chose a 50 mm × 0.1 mm × 50 mm photorefractive polymer (Nitto Denko Technical) as the PCM, for its long hologram persistency under R^*. A more detailed description of the experimental setup is available in the literature [11].

During the experiment, the CCD, whose gating width was set at 50 ms, captured three images: the fluorescent light distribution excited by the sample beam (DC, figure 2(b)), the phase conjugated beam of the unmodulated photons when the sample beam was frequency shifted to f_0 (TRDC, figure 2(c)),

and the phase conjugated beam of the modulated photons when the sample beam was frequency shifted to f_0–f_{US} (TRUE, figure 2(d)). Each of the fluorescence images was normalized to its maximum intensity. For the TRDC and TRUE images, the background signal due to the randomly scattered R^* from the photorefractive polymer had already been removed by subtracting the fluorescence image when no stable hologram was formed and no phase conjugated beam was generated (supplementary figure 1 available at stacks. iop.org/LPL/10/075604/mmedia). Figure 2(e) compares the spatial extent of the excited fluorescence signals along the bar length under the DC, TRDC and TRUE light excitations. As seen, compared with the DC and TRDC light, the TRUE light excited a substantially smaller range of the fluorescent bar, which was ∼1 mm in FWHM—approximately the ultrasound focal width divided by $\sqrt{2}$ [9, 20]. Note that only part of the optical modes from the experimental sample was collected onto the PCM, and the consequent imperfect phase conjugation led to some intensity offset, as seen in our TRUE images. This offset, however, did not blur the optical focusing in our system as much as in the digital TRUE approach [12], because far fewer independent optical modes were phase conjugated from the SLM there.

To demonstrate the dynamic focusing ability of TRUE focusing, we scanned the US focal position along the
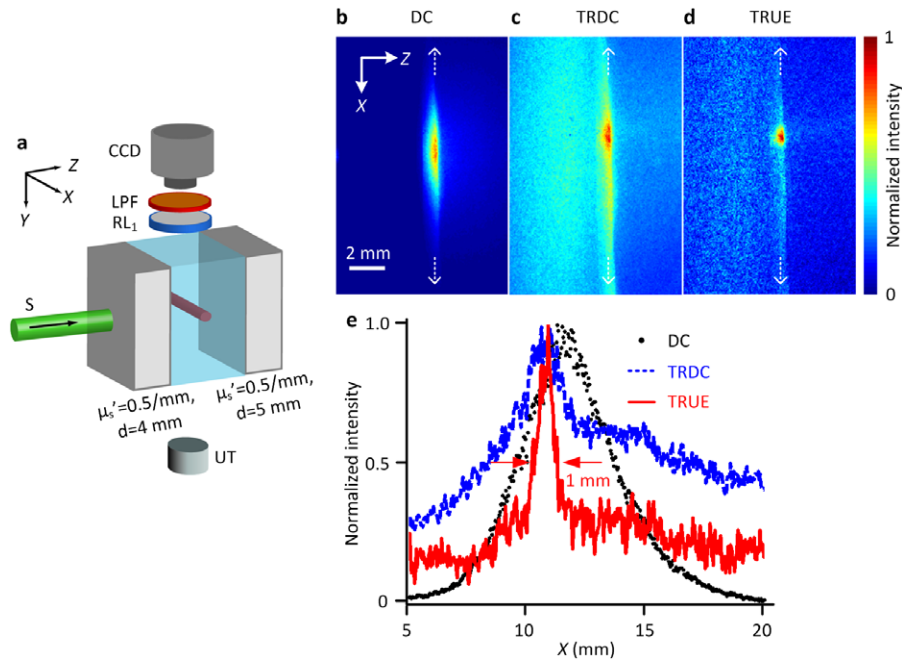
Figure 2. Direct visualization of TRUE optical focusing within thick turbid media. (a) Illustration of the sample arrangement. A fluorescent bar was embedded centrally inside a transparent gel sandwiched between two scattering layers. The center of the US focus was aligned to intercept the center of the fluorescent bar in both the *Y* and *Z* directions. (b)–(d) CCD images of the fluorescence emission under the illuminations of (b) the incident sample beam (DC), (c) the phase conjugated beam of the unmodulated photons (TRDC) and (d) the tightly focused phase conjugated beam of the modulated photons (TRUE). (e) Intensity distributions of fluorescence signals excited by the DC, TRDC and TRUE light along the white dashed lines in (b)–(d), respectively.

X direction, while keeping the sample and the optical components stationary. At each position, we obtained three fluorescence images, excited by the DC, TRDC and TRUE light, respectively. As shown in supplementary movie 1 (available at stacks.iop.org/LPL/10/075604/mmedia), the peak position of the TRUE fluorescence emission tracks the ultrasound focal position along the *X* direction, while the DC and TRDC emissions do not.

To demonstrate the capability of focused fluorescence imaging in turbid media, we prepared another experimental sample, as shown in figure 3(a), to use with a system that employs a 10 mm × 10 mm × 5 mm $Bi_{12}SiO_{20}$ (BSO, Elan) as the PCM. This material was chosen for its faster response time, to improve the system's immunity to environmental vibrations and US-induced speckle decorrelation. With the same aim, the US beam in this study functioned in a burst mode with a duty cycle of 20%, and the peak-to-peak focal pressure was decreased to 0.9 MPa. To ensure good acoustic coupling for ultrasonic wave propagation, an 8 mm-thick turbid layer was surrounded by two transparent layers in the *Z* direction and water in the *Y* direction. On the mid-*Z* plane of this scattering layer, two objects ($2 \times 2 \times 1$ mm^3), dyed with 2.8×10^{-7} μM of 2 μm diameter polystyrene fluorescent microspheres (F8825, Invitrogen), were placed with a separation of 4.5 and 10 mm beneath the sample's top surface. Also, we embedded two pencil lead refills (0.5 mm diameter) to aid pre-alignment so that the US focus could traverse the center of the two targets in both the *Y* and *Z* directions when the sample was scanned in the *X* direction. The scanning step size was 0.2 mm, and at each *X* position

an avalanche photodiode (SPM3Q-T, Newport) detected three fluorescence signals under different conditions: a DC signal excited by the sample beam, a TRDC signal excited by the phase conjugated unmodulated diffused light and a TRUE signal excited by the phase conjugated modulated diffused light. We also measured a background signal, the fluorescence excitation by the scattered reading beam. The TRDC and TRUE signals were obtained by subtracting this background signal (supplementary figure 2 available at stacks.iop.org/LPL/10/075604/mmedia).

Figure 3(b) shows the distribution of normalized fluorescence signal intensities at different sample *X* positions. As shown, the fluorescent DC and TRDC light lacked the spatial resolution needed to resolve the two closely positioned fluorescent targets, since they were excited by unfocused diffused light. In contrast, the fluorescent TRUE light had sufficient resolution to clearly depict the size and the position of these two targets: in the image, both appear ~2 mm (FWHM) wide and are separated by 4.7 mm, agreeing well with the sample arrangements. Moreover, the imaging resolution, obtained from a Gaussian fit to the TRUE profile, was about 0.9 mm, which is close to the size of the fluorescently excited area observed in figure 2. In comparison, figure 3(c) shows the DC, TRDC and TRUE images acquired by PD$_1$ and PD$_2$ (figure 1(c)), based on the absorption contrast of 532 nm light by the dyed objects (see supplementary figure 3 available at stacks.iop.org/LPL/10/075604/mmedia for examples of signal processing). Since the fluorescence emission originates from the absorbance of 532 nm light, the images in figures 3(b) and (c) are
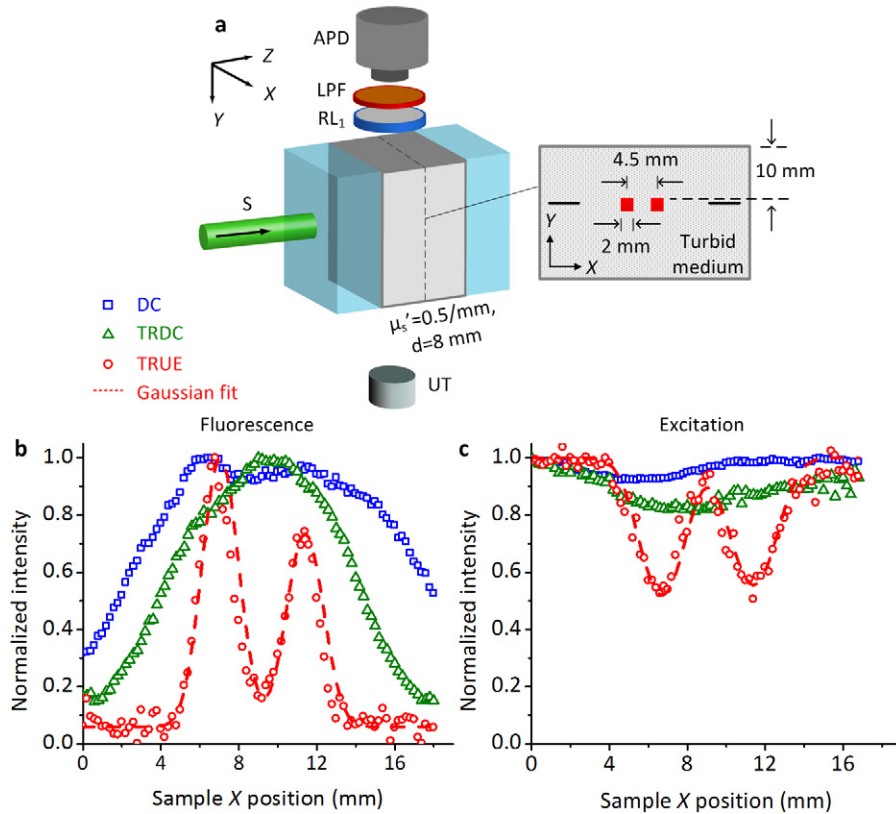
Figure 3. Fluorescence imaging of small objects embedded inside a thick turbid medium. (a) Illustration of sample arrangement. (b) Comparison of fluorescence images excited by the DC, TRDC and TRUE light, respectively. (c) Comparison of DC, TRDC and TRUE images based on the absorption contrast of 532 nm excitation light. The discrete symbols in (b) and (c) represent the experimental data, and the dashed curves represent Gaussian fits to the TRUE measurements.

complementary to each other. Moreover, these two sets of measurements are consistent in terms of spatial resolution: objects that cannot be resolved in the DC or TRDC images can be characterized sharply and accurately by the TRUE images. This, once again, highlights that the 532 nm TRUE light and the consequent fluorescence excitation are both confined within the US focus, which enables focused fluorescence imaging in thick turbid media (∼4 and ∼5 transport mean free paths (TMFPs), along Z and Y, respectively).

3. Discussion

Delivery or excitation of tightly focused light deep in turbid media (such as biological tissue) beyond the optical ballistic regime has been the goal of intensive investigations. The TRUE optical focusing method recently invented by Xu *et al* [9] has rapidly attracted much attention [10–13, 20, 21] as it uniquely creates a virtual guide star for dynamic optical focusing inside turbid media. In this letter, with TRUE systems that use either a photorefractive polymer or a BSO crystal as the PCM, we successfully established a straightforward visualization of optical focusing inside turbid media with thicknesses of more than four TMFPs. We further showed that, with reduced speckle decorrelation caused by the continuous and long bursts of US beams, the optical focus was confined within the US focus, so that the optical focus could be dynamically guided wherever the US focus was

moved within the optical sensing region. To exemplify the broad potential of TRUE, we also demonstrated that the TRUE light can be used for focused fluorescence imaging with an ultrasonically determined spatial resolution deep inside turbid media.

The current study was limited in the two-dimensional (XZ plane) investigation of optical focusing because the use of continuous or long bursts of US beams yielded poor spatial resolution along the acoustic axis. However, pumping the acousto-optic interaction with a short pulsed laser source, as described in the literature [12, 13], would enable the usage of short US pulses with a high focal pressure, while retaining sufficient US-modulated photons to record the phase hologram inside the photorefractive material within a short period of time. Thus, during the holographic reading stage, an improved axial resolution of optical focus can be attained inside turbid media. Moreover, the reported investigations with analogue PCM-based TRUE have been performed inside turbid media with optical thicknesses of less than 20 TMFPs, and refocusing to a pixel in space required 200 ms for recording the hologram and 10 ms for reading the hologram, durations largely restricted by the response time of the photorefractive materials. Even though this is already >30 times faster than the state-of-the-art digital TRUE system [12], transition to pulsed laser and ultrasound sources would boost the number of instantaneous US-modulated photons [12, 13, 22] and accelerate the

photorefractive response to less than 1 ms [17, 23, 24]. Finally, the use of short pulsed ultrasound would bestow a much higher FBR [8], which is highly desired for focusing. Thus, our analogue approach to TRUE optical focusing has the potential to penetrate more sharply and deeply into biological tissue and operate in real time. These capabilities could spur a wide range of *in vivo* biomedical applications, including optical manipulation, imaging and therapy.

Acknowledgments

References

[1] Tuchin V 2007 *Tissue Optics: Light Scattering Methods and Instruments for Medical Diagnosis* 2nd edn (Bellingham, WA: SPIE Optical Engineering Press)

[2] Wang L V and Wu H 2007 *Biomedical Optics: Principles and Imaging* (Hoboken, NJ: Wiley)

[3] Ntziachristos V 2010 Going deeper than microscopy: the optical imaging frontier in biology *Nature Methods* **7** 603–14

[4] Fisher R A 1983 *Optical Phase Conjugation* (New York: Academic)

[5] Yaqoob Z, Psaltis D, Feld M S and Yang C 2008 Optical phase conjugation for turbidity suppression in biological samples *Nature Photon.* **2** 110–5

[6] Aulbach J, Gjonaj B, Johnson P M, Mosk A P and Lagendijk A 2011 Control of light transmission through opaque scattering media in space and time *Phys. Rev. Lett.* **106** 103901

[7] Katz O, Small E, Broomberg Y and Silberberg Y 2011 Focusing and compression of ultrashort pulses through scattering media *Nature Photon.* **5** 372–7

[8] Mosk A P, Lagendijk A, Lerosey G and Fink M 2012 Controlling waves in space and time for imaging and focusing in complex media *Nature Photon.* **6** 283–92

[9] Xu X, Liu H and Wang L V 2011 Time-reversed ultrasonically encoded optical focusing into scattering media *Nature Photon.* **5** 154–7

[10] Lai P, Xu X, Liu H, Suzuki Y and Wang L V 2011 Reflection-mode time-reversed ultrasonically encoded (TRUE) optical focusing into turbid media *J. Biomed. Opt.* **16** 080505

[11] Suzuki Y, Xu X, Lai P and Wang L V 2012 Energy enhancement in time-reversed ultrasonically encoded optical focusing using a photorefractive polymer *J. Biomed. Opt.* **17** 080507

[12] Wang Y M, Judkewitz B, DiMarzio C A and Yang C 2012 Deep-tissue focal fluorescence imaging with digitally time-reversed ultrasound-encoded light *Nature Commun.* **3** 928

[13] Si K, Fiolka R and Cui M 2012 Fluorescence imaging beyond the ballistic regime by ultrasound-pulse-guided digital phase conjugation *Nature Photon.* **6** 657–61

[14] Hariharan P 2002 *Basics of Holography* (Cambridge: Cambridge University Press)

[15] Lev A and Sfez B G 2003 *In vivo* demonstration of the ultrasound-modulated light technique *J. Opt. Soc. Am.* A **20** 2347–54

[16] Draijer M, Hondebrink E, van Leeuwen T and Steenbergen W 2009 Review of laser speckle contrast techniques for visualizing tissue perfusion *Lasers Med. Sci.* **24** 639–51

[17] Solymar L, Webb D J and Jepsen A G 1996 *The Physics and Applications of Photorefractive Materials* (*Oxford Series in Optical and Imaing Sciences*) (Oxford: Clarendon)

[18] Gunter P and Huignard J P (ed) 2006 *Photorefractive Materials and Their Applications 1: Basic Effects* (New York: Springer)

[19] 2000 *American National Standard for the Safe Use of Laser in Health Care Facilities, ANSI Z1361.1* (New York: American National Standards Institute)

[20] Liu H, Xu X, Lai P and Wang L V 2011 Time-reversed ultrasonically encoded (TRUE) optical focusing into tissue-mimicking media with optical thickness up to 70 *J. Biomed. Opt.* **16** 086009

[21] Lai P, Xu X, Liu H and Wang L V 2012 Time-reversed ultrasonically encoded (TRUE) optical focusing in biological tissue *J. Biomed. Opt.* **17** 030506

[22] Rousseau G, Blouin A and Monchalin J-P 2008 Ultrasound-modulated optical imaging using a powerful long pulse laser *Opt. Express* **16** 12577–90

[23] Valley G C, Klein M B, Mullen R A, Rytz D and Wechsler B 1988 Photorefractive materials *Annu. Rev. Mater. Sci.* **18** 165–88

[24] Jones D C and Solymar L 1991 Transient response of photorefractive bismuth silicon oxide in the pulsed regime *Opt. Commun.* **85** 372–80